Available online at www.sciencedirect.com
ScienceDirect
Journal of Solid State Chemistry 181 (2008) 306–312
JOURNAL OF SOLID STATE CHEMISTRY
www.elsevier.com/locate/jssc

Ordered distribution of I and Cl in the low-temperature crystal structure of mutnovskite, $Pb_4As_2S_6ICl$: An X-ray single-crystal study

Luca Bindi[a], Anna Garavelli[b], Daniela Pinto[b,*], Giovanni Pratesi[a,c], Filippo Vurro[b]

[a]*Museo di Storia Naturale, Sezione di Mineralogia, Università degli Studi di Firenze, Via La Pira, 4-I-50121 Firenze, Italy*
[b]*Dipartimento Geomineralogico, Università degli Studi di Bari, Via E. Orabona 4, I-70125 Bari, Italy*
[c]*Dipartimento di Scienze della Terra, Università degli Studi di Firenze, Via La Pira, 4-I-50121 Firenze, Italy*

Received 11 October 2007; received in revised form 20 November 2007; accepted 25 November 2007
Available online 4 December 2007

Abstract

To study the temperature-dependent structural changes and to analyze the crystal chemical behavior of the halogens as a function of temperature, a crystal of the recently discovered mineral mutnovskite, ideally $Pb_2AsS_3(I,Cl,Br)$, has been investigated by X-ray single-crystal diffraction methods at 300 and 110 K. At room temperature (RT) mutnovskite was confirmed to possess a centrosymmetric structure-type, space group *Pnma*, while at low temperature (110 K) it adopts a non-centrosymmetric orthorhombic structure-type, space group $Pnm2_1$, with $a = 11.5394(9)$ Å, $b = 6.6732(5)$ Å, $c = 9.3454(7)$ Å, $V = 719.64(9)$ Å^3 and $Z = 2$. Mutnovskite reconverts to the centrosymmetric-type upon returning to RT thus indicating that the phase transition is completely reversible in character. The refinement of the LT-structure leads to a residual factor $R = 0.0336$ for 1827 independent observed reflections [$F_o > 4\sigma(F_o)$] and 80 variables. The crystal structure of cooled mutnovskite is topologically identical to that observed at RT and the slight structural changes occurring during the phase transition $Pnma \rightarrow Pnm2_1$ are mainly restricted to the coordination polyhedra around Pb. The structure solution revealed that I and Cl are ordered into two specific sites. Indeed, the unique mixed (I,Cl) position in the RT-structure (Wyckoff position 4*c*) transforms into two 2*a* Wyckoff positions in the LT-structure hosting I and Cl, respectively.

Keywords: Mutnovskite; Phase transition; LT-structure; I–Cl ordering

1. Introduction

Mutnovskite, ideally $Pb_2AsS_3(I,Cl,Br)$, is an interesting halogen sulfosalt recently discovered from the high-temperature fumarole field of the Mutnovsky volcano, Kamchatka Peninsula, Russian Federation [1]. The most interesting feature of mutnovskite is the presence of iodine, which so far has not been found in this type of minerals, and allows to consider mutnovskite as the first representative of the new class of I-bearing sulfosalts [2]. Microprobe measurements gave the average empirical formula: $Pb_{1.99}(As_{0.98}Bi_{0.02})_{\Sigma 1.00}(S_{2.98}Se_{0.02})_{\Sigma 3.00}(I_{0.47}Cl_{0.46}Br_{0.09})_{\Sigma 1.02}$. The crystal structure of mutnovskite was solved and refined in the space group *Pnma* [1]. It consists of three independent cation sites: Pb1 and Pb2 in tricapped trigonal prismatic coordination with S and I(Cl) atoms (completed with one As atom in the case of Pb2) and As in threefold coordination with S atoms which form the base of a trigonal pyramid with As at the apex. In the crystal structure of mutnovskite, the two halogens I and Cl are located in a unique mixed position labeled X, with approximately equal occupancy each. Small amount of Br (~0.09 apfu) has been supposed to host the same position as well [1].

The occurrence of I together with Cl and/or Br is well known among some mercury halogen sulfides of the capgaronnite–perroudite group [3]. However, in each of these minerals I and Cl occupy distinct structure positions and at most Br → I or Br → Cl substitutions were observed in some minerals such as perroudite $Hg_5Ag_4S_5(Cl,Br,I)_4$ [4] and capgaronnite HgAg(Cl,Br,I) [5]. The presence in mutnovskite of I and Cl coexisting in the same structural site is then very remarkable. In addition, the almost equal

*Corresponding author. Fax: +39 80 5442591.
E-mail address: d.pinto@geomin.uniba.it (D. Pinto).

0022-4596/$ - see front matter © 2007 Elsevier Inc. All rights reserved.
doi:10.1016/j.jssc.2007.11.032

occupancy of Cl and I in the *X* site appears to suggest the wish of the structure to order these two halogens. In this light, we decided to study the temperature-dependent structural changes in mutnovskite and to verify the possibility of halogen ordering at low temperature. For this purpose, a single-crystal X-ray diffraction study at low temperature (ca. 110 K), as well as microprobe investigations, have been performed herein on a crystal of mutnovskite from the type locality.

2. Experimental

Several crystals of mutnovskite were selected from the 7/nm (V28) sample (Mineralogical Collection of the Museum "C.L. Garavelli", Dipartimento Geomineralogico, Università di Bari) and examined by means of a Bruker P4 single-crystal diffractometer using graphite-monochromatized Mo$K\alpha$ radiation and with an Oxford Diffraction Xcalibur 2 diffractometer (Enhance X-ray source, X-ray Mo$K\alpha$ radiation, $\lambda = 0.71073$ Å), fitted with a Sapphire 2 CCD detector. A crystal of relatively high diffraction quality was selected for the structural study. A preliminary chemical analysis performed on the selected crystal by using energy-dispersive spectrometry (EDS), did not indicate the presence of elements ($Z > 9$) other than Pb, As, S, I, Cl and very minor Se. The chemical composition was then determined using wavelength dispersive analysis (WDS) by means of a Jeol JXA-8600 electron microprobe. The operating conditions were: accelerating voltage 15 kV, beam current 20 nA; standards (element, *emission line*, counting time for one spot analysis): galena (Pb$M\alpha$, 20 s); marcasite (Fe$K\alpha$, 40 s; S$K\alpha$, 20 s); iodargyrite (I$L\alpha$, 20 s); tugtupite (Cl$K\alpha$, 20 s); synthetic GaAs (As second order $L\alpha$, 40 s); synthetic Bi_2Se_3 (Bi$M\alpha$, 40 s; Se second order $L\alpha$, 40 s), covellite (Cu$K\alpha$, 40 s), pure Tl (Tl$M\alpha$, 40 s), and bromargyrite (Br second order $L\alpha$, 40 s). The estimated analytical precision (in wt%) is: ±0.60 for Pb, ±0.50 for I; ±0.30 for Bi, Cl, and Br; ±0.20 for As and S; ±0.10 for Se; and ±0.05 for Fe, Cu, and Tl. The investigated crystal was found to be homogeneous within the analytical uncertainty. The average chemical composition (seven analyses on different spots) is reported in Table 1. On the basis of $\Sigma_{atoms} = 14$, the empirical chemical formula for the selected mutnovskite crystal is $Pb_{4.00}(As_{1.96}Bi_{0.04})_{\Sigma=2.00}(S_{5.91}Se_{0.10})_{\Sigma=6.01}I_{1.00}Cl_{0.98}$. In spite of the composition of the holotype of mutnovskite, no bromine content was found in the crystal analyzed in this item.

A first room temperature (RT, ca. 300 K) X-ray diffraction data collection was carried out with the Oxford Diffraction Xcalibur 2 single-crystal diffractometer. To verify the possibility of ordering between I and Cl into two independent positions (*vide supra*), a second measurement was performed at ca. 110 K on the same crystal with the same instrument, the low temperature being achieved by means of an Oxford cryostream cooler. Before the measurement, the sample was held at the specified temperature for about 180 min. A relatively high $\sin(\theta)/\lambda$ cutoff and a high redundancy were chosen in the recording setting design to account for a potential reduction of symmetry in the low-temperature structure of mutnovskite (hereafter LT-structure). After the cooling experiment, the crystal was re-heated again at 300 K and a new data collection was done. The unit-cell values obtained did not reveal significant variation from the previous one and the structure showed its original centrosymmetric arrangement (*vide infra*). In order to control the role of the kinetics in reaching equilibrium, the crystal was kept at 110 K for 48 h, and the unit-cell values were determined again. No appreciable time-dependent change in intensities and/or positions of the reflections was observed.

Table 1
Electron microprobe data and atomic ratios, on the basis of $\Sigma_{atoms} = 14$, for the selected mutnovskite crystal

	wt%	Range	Atomic ratios
Pb	61.67	61.22–62.04	4.00
Fe	0.01	0.00–0.02	0.00
Cu	0.01	0.00–0.02	0.00
Bi	0.62	0.50–0.69	0.04
As	10.95	10.66–11.03	1.96
Tl	0.01	0.00–0.02	0.00
S	14.11	13.98–14.28	5.91
Se	0.59	0.44–0.67	0.10
Cl	2.59	2.47–2.65	0.98
I	9.47	9.37–9.60	1.00
Br	0.01	0.00–0.02	0.00
Total	100.04	99.78–100.29	

Intensity integration and standard Lorentz-polarization correction were performed with the CrysAlis software package [6]. The empirical method proposed by Blessing [7] was applied for the absorption correction.

2.1. Structure refinement at 300 K

The values of the equivalent pairs were averaged. The merging R for the ψ-scan data set decreased from 0.1427 before absorption correction to 0.0391 after this correction. Systematic absences ($0\,k\,l$: $k+l=2n$; $h\,k\,0$: $h=2n$; $h\,0\,0$: $h=2n$; $0\,k\,0$: $k=2n$; $0\,0\,l$: $l=2n$) are consistent with the space groups $Pn2_1a$ ($Pna2_1$ as standard) and *Pnma*. Statistical tests on the distribution of $|E|$ values strongly indicate the presence of an inversion center [$|E^2-1| = 0.956$], thus confirming the space group *Pnma* for the room-temperature structure of mutnovskite. The structure refinement was performed starting from the model obtained for the RT-structure of mutnovskite [1], using the program SHELXL-97 [8]. Convergence was rapidly obtained to a final R index of 0.0362 for 1899 observed reflections [$F_o > 4\sigma(F_o)$]. The results of the RT structure are essentially identical to those reported by Zelenski et al. [1] in the original description of mutnovskite, and for this reason they are not reported herein.

2.2. Structure determination and refinement at 110 K

The values of the equivalent pairs were averaged. The merging R for the ψ-scan data set decreased from 0.1988 before absorption correction to 0.0903 after this correction. The analysis of the systematic absences ($0\,k\,l$: $k+l=2n$; $0\,k\,0$: $k=2n$; $0\,0\,l$: $l=2n$) are consistent with the space groups $Pnm2_1$ ($Pmn2_1$ as standard), $Pn2_1m$ ($Pmn2_1$ as standard) and $Pnmm$ ($Pmmn$ as standard). Statistical tests on the distribution of $|E|$ values strongly indicate the absence of an inversion center [$|E^2-1|=0.708$], thus suggesting the choice of the space group $Pnm2_1$ or $Pn2_1m$. It is worth noting that the $h\,k\,0$ reflections having $h=2n+1$ are present at low temperature, thus implying the loss of the glide plane a of the RT-structure. To decide the correct space group for the LT-structure we analyzed the maximum orthorhombic *translationengleiche* subgroups of the $Pnma$ space group. They are: $Pn2_1a$, $Pnm2_1$, $P2_1ma$, and $P2_12_12_1$. Hence, the correct space group for the LT-structure of mutnovskite is $Pnm2_1$. We decided to solve the structure in the non-standard space group $Pnm2_1$ in order to maintain the original orientation (*vide infra*).

Table 2
Data and experimental details at low temperature for the selected mutnovskite crystal

Crystal data	
X-ray formula	$Pb_4As_2S_6ICl$ [Pb_2AsS_3(I,Cl,Br)][a]
Cell setting	Orthorhombic [orthorhombic][a]
Space group	$Pnm2_1$ [$Pnma$][a]
a (Å)	11.5394(9) [11.543(1)][a]
b (Å)	6.6732(5) [6.6764(7)][a]
c (Å)	9.3454(7) [9.359(1)][a]
V (Å^3)	719.64(9) [721.3(1)][a]
Z	2 [4][a]
Data collection	
Radiation type	Mo$K\alpha$ (graphite monochromator)
Temperature	110 K
Detector to sample distance	4 cm
Crystal size	$0.022\times0.030\times0.032$ mm^3
Active detection-area	6.25×6.25 cm^2
Resolution	512×512 pixels
Number of frames	2954
Rotation width per frame	0.15°
Measuring time	240 s
Maximum covered 2θ	56.64° ($d=0.75$ Å)
Unique reflections	1915
Reflections $I>2\sigma_I$	1827
R_{int} before absorption correction	0.1988
R_{int} after absorption correction	0.0903
R_σ	0.0525
Range of h, k, l	$-15\leqslant h\leqslant15$, $-8\leqslant k\leqslant8$, $-12\leqslant l\leqslant11$
Refinement	
R [$F_o>4\sigma$ (F_o)]	0.0336
R (all data)	0.0341
Goof	1.187
Number of least squares parameters	80

[a]Crystal data for the room-temperature structure of mutnovskite [1].

The position of most of the atoms was determined from the three-dimensional (3D) Patterson synthesis [9]. A least-squares refinement (by means of the program SHELXL-97 [8]) using these heavy-atom positions and isotropic temperature factors yielded an R factor of 0.1288. The 3D difference Fourier synthesis yielded the position of the remaining sulfur atoms, as well as of the halogens. The introduction of anisotropic temperature factors for all the atoms led to $R=0.0336$ for 1827 observed reflections [$F_o>4\sigma(F_o)$] and $R=0.0341$ for all 1915 independent reflections. Neutral scattering factors for Pb, As, I, Cl, and S were taken from the *International Tables for* X-ray *Crystallography* [10]. The solution revealed that in the LT-structure of mutnovskite I and Cl are ordered into two specific sites. Indeed, the unique mixed (I,Cl) position in the RT-structure (Wyckoff position 4c) transforms into two 2a Wyckoff positions in the LT-structure hosting I and Cl, respectively. The attempt to refine the occupancy of the I site (I vs. vacancy) and Cl site (Cl vs. vacancy) produced values consistent with pure I and Cl, respectively. Inspection of the difference Fourier map revealed that maximum positive and negative peaks were 3.17 and 2.78 e$^-$/Å^3, respectively. Experimental details and R indices are given in Table 2. Fractional atomic coordinates and anisotropic-displacement parameters are shown in Table 3. Supplementary table lists the observed and calculated structure factors.

3. Description of the low-temperature structure

The present study showed that the atomic arrangement of mutnovskite at low temperature is topologically identical to that of the RT-structure of mutnovskite. However, in the LT-structure the two halogens, Cl and I, are ordered into two specific sites (Fig. 1). This leads to a reduction of symmetry from the centrosymmetric space group $Pnma$ to the non-centrosymmetric $Pnm2_1$. Hence, the LT-structure consists of 12 independent atom positions (six cation sites and six anion sites) instead of six as in the RT-mutnovskite. The two cation sites Pb1 and Pb3 show a distorted tricapped trigonal prismatic coordination very similar to that of Pb1 in the RT-mutnovskite. Pb1 is coordinated by six S atoms (2.753–3.638 Å), two Cl atoms (3.575 Å) and one I atom (3.345 Å), Pb3 by six S atoms (2.769–3.631 Å), two I atoms (3.570 Å) and one Cl atom (3.334 Å). Analogously, the two sites Pb2 and Pb4 are similar to the site Pb2 in the RT-structure and their coordination has the form of a bicapped trigonal prism (or tricapped if the closest As atom is included in the coordination). Pb2 is coordinated by six S atoms (2.905–3.447 Å), one Cl atom (3.034 Å) and one I atom (3.438), Pb4 by six S atoms (2.894–3.442 Å), one I atom (3.047 Å) and one Cl atom (3.472 Å). The selected values of bond lengths match closely those observed for the corresponding Pb coordinations in the structure of the RT-mutnovskite (Table 4). An exception is represented by the Pb3–Cl and Pb4–Cl distances which are, respectively,

Table 3
Fractional atomic coordinates and anisotropic displacement parameters U_{ij} (Å^2) for the crystal structure of mutnovskite at low temperature

Site	x	y	z	U_{11}	U_{22}	U_{33}	U_{23}	U_{13}	U_{12}	U_{eq}
Pb1	0.37479(6)	0	0.2047(1)	0.0491(4)	0.0492(4)	0.0502(5)	0	−0.0001(3)	0	0.0495(3)
Pb2	0.07790(6)	$\frac{1}{2}$	0.29669(8)	0.0467(4)	0.0462(4)	0.0479(4)	0	−0.0004(3)	0	0.0469(2)
Pb3	0.87500(7)	0	0.3210(1)	0.0513(4)	0.0509(4)	0.0527(5)	0	0.0001(3)	0	0.0516(3)
Pb4	0.42176(6)	0	0.73070(8)	0.0483(4)	0.0480(4)	0.0502(4)	0	0.0008(3)	0	0.0488(2)
As1	0.3277(2)	$\frac{1}{2}$	0.4776(2)	0.0417(8)	0.0428(9)	0.045(1)	0	−0.0005(8)	0	0.0431(4)
As2	0.1705(2)	0	0.5479(2)	0.0394(8)	0.0412(9)	0.0430(9)	0	0.0013(7)	0	0.0412(4)
I	0.20412(9)	0	0.9154(1)	0.0385(4)	0.0386(4)	0.0405(5)	0	−0.0004(4)	0	0.0392(3)
Cl	0.2935(3)	$\frac{1}{2}$	0.1108(5)	0.040(2)	0.037(2)	0.038(2)	0	0.001(2)	0	0.0383(7)
S1	0.1520(4)	0	0.3101(6)	0.037(1)	0.039(2)	0.043(2)	0	0.002(2)	0	0.0395(9)
S2	0.4529(3)	0.7491(4)	0.4315(5)	0.047(1)	0.048(1)	0.050(2)	−0.001(2)	−0.001(1)	−0.001(1)	0.0481(6)
S3	0.3495(4)	$\frac{1}{2}$	0.7164(6)	0.041(2)	0.043(2)	0.045(3)	0	−0.002(2)	0	0.0431(9)
S4	0.0460(3)	0.2505(4)	0.5937(5)	0.048(1)	0.049(1)	0.051(2)	−0.002(1)	0.001(2)	0.001(1)	0.0497(6)

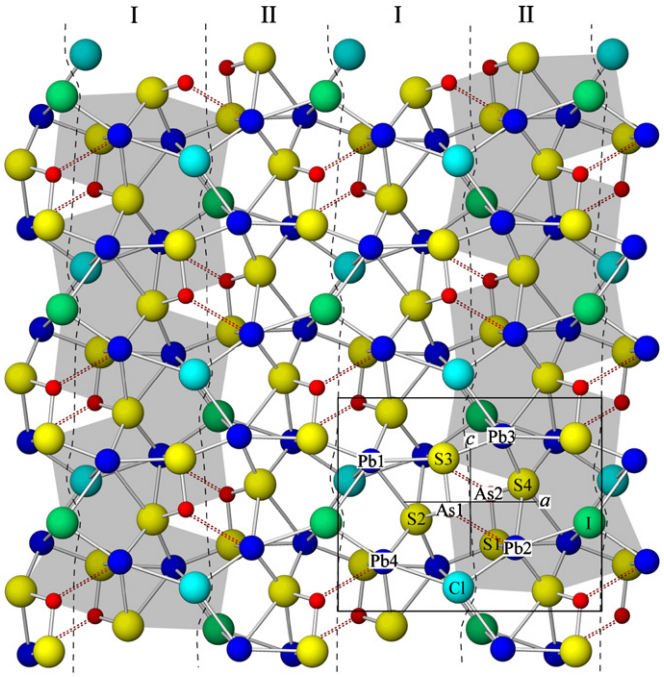

Fig. 1. The crystal structure of mutnovskite at low temperature projected on (010). Dark-blue: Pb atoms; red: As atoms; light blue: Cl atoms; green: I atoms; and yellow: S atoms. The unit cell is displaced by $-\frac{1}{2}a$, $-\frac{1}{2}b$, $-\frac{1}{2}c$. Dark dashed lines: limits of layers parallel to (100); red dashed lines: connection from Pb atoms to the closest As atoms, which form the missing vertex of the prism. Columns of Pb1 and Pb4 (layer I) and Pb2 and Pb3 (layer II) are shaded on the left- and right-hand side, respectively.

Table 4
Interatomic distances (Å) and s.u.'s for the LT-structure and RT-structure of mutnovskite

LT-mutnovskite		RT-mutnovskite	
Pb1−S1	2.753(5)	Pb1−S2	2.760(5)
Pb1−S2 (×2)	2.847(4)	Pb1−S1 (×2)	2.853(3)
Pb1−S3	3.183(5)	Pb1−S2	3.194(5)
Pb1−I	3.345(1)	Pb1−X	3.354(2)
Pb1−Cl (×2)	3.575(2)	Pb1−X (×2)	3.570(1)
Pb1−S2 (×2)	3.638(4)	Pb1−S1 (×2)	3.636(4)
Pb3−S3	2.769(5)		
Pb3−S4 (×2)	2.849(4)		
Pb3−S1	3.198(5)		
Pb3−Cl	3.334(4)		
Pb3−I (×2)	3.570(1)		
Pb3−S4 (×2)	3.631(4)		
Pb2−S4 (×2)	2.905(4)	Pb2−S1 (×2)	2.906(3)
Pb2−Cl	3.034(4)	Pb2−X	3.047(4)
Pb2−S4 (×2)	3.258(4)	Pb2−S1 (×2)	3.269(4)
Pb2−I	3.438(1)	Pb2−X	3.445(2)
Pb2−S1 (×2)	3.447(1)	Pb2−S2 (×2)	3.446(1)
Pb4−S2 (×2)	2.894(4)		
Pb4−I	3.047(1)		
Pb4−S2 (×2)	3.279(4)		
Pb4−Cl	3.472(4)		
Pb4−S3 (×2)	3.442(1)		
As1−S2 (×2)	2.244(3)	As−S1 (×2)	2.241(3)
As1−S3	2.246(6)	As−S2	2.245(5)
As2−S1	2.233(6)		
As2−S4 (×2)	2.245(3)		

shorter and longer than the corresponding Pb–X (X = Cl, I, Br) distances in the RT-structure. Moreover, due to the cooling, a minor shortening of some of the other cation-to-anion distances is observed as well (Table 4). This is reflected in the reduction of the lattice parameters (Table 2), which testifies for the overall contraction of the mutnovskite structure at low temperature.

As shown by Zelenski et al. [1] the crystal structure of mutnovskite has a layered character with layers parallel to (100). In the RT-structure each layer consists of pairs of Pb1 and Pb2 prisms connected in columns which extend along **c** and are laterally connected through Pb–S bonds with the adjacent layers. In the case of the LT-structure two kinds of layers alternating along **a** are present instead of one. The former (layer I) contains only Cl atoms and is formed by pairs of Pb1 and Pb4 prisms connected in columns parallel to [001], the latter (layer II) contains only I atoms and is formed by columns of Pb2 and Pb3 prisms (Fig. 1); the internal geometry of the two layers in the LT-structure is the same as that of layers in the RT-structure.

As in the RT-structure, two kinds of channels running parallel to [010] occur between the layers: the smaller

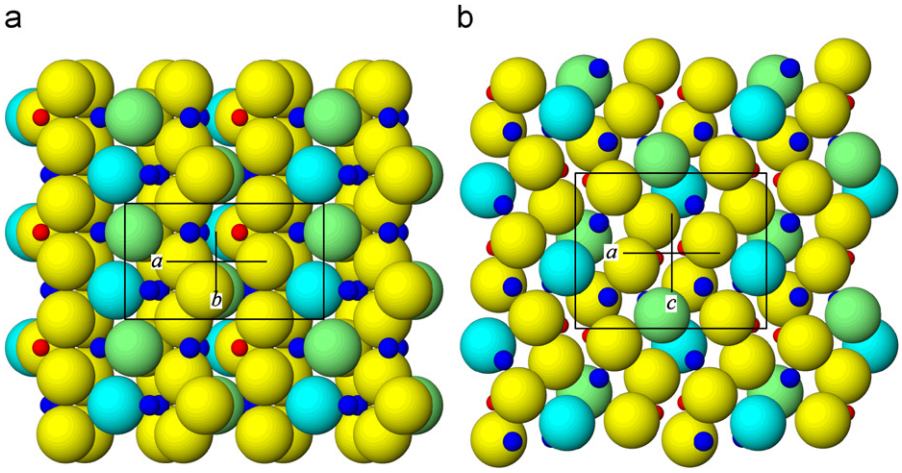

Fig. 2. [010] channels of alternating I and Cl atoms in the crystal structure of mutnovskite at low temperature: (a) view along [001] and (b) view along [010]. Light blue: Cl atoms; green: I atoms; yellow: S atoms; dark-blue: Pb atoms; and red: As atoms.

Table 5
Coordination parameters[a] for cation sites for the crystal structure of mutnovskite at low temperature

Site	Coordination	$\langle d \rangle$	d_{min}	d_{max}	V_s	ECC_L	SPH_L	V_p	υ	Valence[b]
Pb1	6S + 2Cl + I	3.3(4)	2.753(5)	3.638(4)	142.61	0.166	0.9463	66.9(1)	0.038	2.10
Pb2	6S + Cl + I	3.2(2)	2.905(4)	3.447(1)	139.37	0.078	0.9448	49.8(1)	0.176	1.66
Pb3	6S + Cl + 2I	3.3(4)	2.769(5)	3.631(4)	142.39	0.163	0.9472	66.8(2)	0.038	2.08
Pb4	6S + Cl + I	3.2(2)	2.894(4)	3.472(4)	140.16	0.083	0.9448	50.3(1)	0.171	1.81
As1	3S	2.245(1)	2.244(3)	2.246(6)	30.22	0.591	1	–	–	3.13
As2	3S	2.241(7)	2.233(6)	2.245(3)	30.50	0.580	1	–	–	3.16

Notes: $\langle d \rangle$ = average bond distance, V_s = volume of the circumscribed sphere, ECC_L = linear eccentricity of the coordination, SPH_L = linear sphericity of the coordination, V_p = volume of the coordination polyhedron, υ = volume distortion.
[a]The polyhedron parameters for atomic coordinations [17,18] were calculated with the program *IVTON* [19].
[b]Bond-valence parameters of Brese and O'Keeffe [20] were used.

channel hosts As atoms close to the channel walls, with their lone-electron pairs occupying the median part, while the larger one accommodates row of alternating halogen and Pb atoms (Fig. 2). The shortening of Pb3–Cl and the stretching of Pb4–Cl with respect to Pb–*X* distances (Table 4), indicate a displacement of Cl atoms towards Pb3 in the structure of LT-mutnovskite and, therefore, towards the inner side of the larger channels accommodating Pb and halogen atoms.

4. Discussion

One of the most interesting result of this study is that the chemical ordering observed in the LT-structure of mutnovskite does not affect significantly the geometry of its coordination polyhedra and of the structure as a whole. This can be well appreciated by the analysis of the coordination parameters reported in Table 5. As a matter of fact, the comparison of the parameters obtained with the values of corresponding cation coordinations in the RT-structure [1] does not show any significant difference. The average between bond-valence of Pb1 and Pb3 is very close to the bond-valence of Pb1 in the RT-mutnovskite (2.09 vs. 2.07, respectively) and the average value Pb2–Pb4 is similar to the bond-valence of Pb2 in the RT-mutnovskite (1.74 vs. 1.77, respectively). In addition, no difference was observed by comparing the coordination environment of the halogen sites into the two structures. As reported above, with the exception of Pb3–Cl and Pb4–Cl, all the selected Pb–Cl and Pb–I bond lengths of the ordered LT-structure of mutnovskite are almost identical to the Pb–*X* distances in the RT-structure. This result is quite unexpected taking into account that *X* is a mixed (I + Cl) site and, therefore, the refined Pb–*X* bond lengths in the RT-structure are only average values of the real Pb–Cl and Pb–I interatomic distances. Due to the larger size of I with respect to Cl, Pb–I distances generally longer than Pb–Cl are expected in the structure in which the two halogens are ordered and occupy two distinct positions. To quote some examples: in cotunnite, $PbCl_2$, the Pb–Cl distances range from 2.85 to 3.63 Å and the two Cl atoms are in four- and five-fold coordination, respectively [11]; Pb–I distances are 3.23 Å in PbI_2 [12] and range from 3.42 to 3.46 Å in Pb(OH)I [13], in both these compounds I atoms are in threefold coordination with Pb forming the base of a trigonal pyramid with I at the apex. On the other hand, the presence of relatively

short distances Pb–I like those in LT-mutnovskite are known in the crystal structure of the heterometallic iodide $PbI_4Cu_2(PPh_3)_4$ [14]. In this compound Pb–I distances range from 2.9895(3) to 3.2186(3) Å.

In spite of the number of natural and synthetic halogen sulfides known, those in which the anionic part involves two halogens, Cl and I, beside sulfur are very scarce. So far, the simultaneous occurrence of both these halogens in the same species has only been reported for mutnovskite and some mercury halogen sulfides such as perroudite $Hg_5Ag_4S_5(Cl,Br,I)_4$ [4], capgaronnite, HgAg(Cl,Br,I)S [5], radtkeite, Hg_3S_2ClI [15], the synthetic $Hg_3S_2BrCl_{0.5}I_{0.5}$ [16]. In these compounds a segregation of I and Cl atoms into structurally different sites is observed, as well as considerable differences in coordination environments about I and Cl, and in *Me*–Cl and *Me*–I distances. In radtkeite, Cl and I atoms show distinct coordinations within similar polyhedron: Cl(1) and I(1) have a distorted three-fold coordination (Hg–Cl = 2.78–3.17 Å; Hg–I = 3.08–3.23 Å) similar to that of I in PbI_2 and Pb(OH)I (the coordination of I may also be described as a square pyramid if the two Hg atoms at 3.41 and 3.48 Å are included in the coordination); Cl(2) and I(2) show an eccentric coordination within an almost distorted triangular prism of six Hg atoms (Hg–Cl = 2.96–3.44 Å; Hg–I = 3.17–3.74 Å), capped with one and three additional Hg atoms, respectively (Hg–Cl = 3.19 Å; Hg–I = 3.17–3.54 Å). In perroudite, Cl is bound preferentially to Hg (Hg–Cl = 3.14–3.34 Å) and its coordination environment has the form of a bicapped trigonal prism if the neighboring Ag atoms are included in the coordination (Ag–Cl = 2.59–3.86 Å); I is preferentially bound to three Ag atoms (Ag–I = 2.74–3.03 Å) forming the base of a distorted trigonal pyramid with I at the apex although three additional weakly bonded Hg atoms (Hg–I5 = 3.46–3.47 Å) are present on the opposite sides of Ag atoms, forming with them a highly distorted octahedral environment around the halogen. In the structure of synthetic $Hg_3S_2BrCl_{0.5}I_{0.5}$ the I atoms have eight Hg neighbors in a square prismatic coordination (Hg–I = 3.26–3.36 Å), whereas Cl atoms are bound to two Hg atoms which are 2.77 and 2.80 Å apart. Pervukhina et al. [15] noted that although a perfect ordering of halogens is observed in this synthetic phase, experiments showed that in synthetic mercury chalcogenide halides, $Hg_3X_2Hal_2$ (X = S, Se, Te; Hal = F, Cl, Br, I) and most likely in minerals [i.e. grechishchevite, $Hg_3S_2(Br,Cl,I)_2$], the Cl:Br:I proportions may change, with statistical occupancies of halogen positions and without changing the integrity of the structure.

In the RT-structure of mutnovskite the coordination of I and Cl does not resemble any of the coordinations described above and no significant differences can be observed between the coordination environment of Cl and I, as well as between between *Me*–Cl and *Me*–I distances. In mutnovskite, indeed, both the halogens, as well as sulfur, show a very distorted and dissymmetric bonding, which may be related to the dissymmetric bonding of Pb and As, induced by the stereochemical activity of their lone electron pair. Tentatively, we may describe the cation environment around Cl and I as a highly distorted trigonal bipyramid.

The similarity of the LT-structure with the RT-structure suggests that the crystal structure of cooled mutnovskite can be interpreted as a "frozen image" of somewhat that would be also ordered at RT. As a matter of fact, the stoichiometric I/Cl atomic ratio (= 1), already observed in the RT-structure, suggests that even at RT there is a constraint in the fixation of the ratio of these two halogens in the crystal structure which, however, is not visible through X-ray single-crystal diffraction. The LT-structure of mutnovskite shows zig-zag columns of Cl and I atoms along **b** (corresponding to equivalent positions in the RT form). Thus, it may signify that, even at RT, I and Cl atoms are strictly ordered in any column, but with two equivalent fillings (i.e. two I–Cl–I–Cl zig-zag chains with 1/2 **b** relative translation), and no ordering between neighboring columns exists. With such a model, X-ray diffraction will only give mean positions and there would be only 1D ordering which may give diffuse streaks for (00*l*) reflections. Nevertheless, no streaks were observed in the diffraction pattern of RT-mutnovskite. If the above hypothesis is exact, the formation of 3D ordering at low temperature would necessitate some mobility of Cl and I atoms along a [010] column. The halogen diffusion within the structure is in fact an asset for the 3D ordering observed in LT-mutnovskite.

5. Conclusions

Our study shows that the crystal structure of cooled mutnovskite ($Pnm2_1$) is very close to that observed at RT ($Pnma$), and that mutnovskite reconverts to the centrosymmetric type upon returning to RT thus indicating that the phase transition is completely reversible in character. We demonstrate by means of an *in situ* data collection at ca. 110 K that the slight structural changes occurring during the phase transformation $Pnma \rightarrow Pnm2_1$ are mainly restricted to the coordination polyhedra around Pb. The AsS_3 pyramid, indeed, is a constant rigid unit in both RT- and LT-structures. However, the slight changes in the Pb coordination polyhedra seem to occur in a continuous way within the temperature range investigated, thus indicating a second-order character of the phase transition. In this way, the RT-structure gradually goes toward the LT-structure without abrupt structural changes.

Acknowledgments

The authors express their gratitude to the three anonymous reviewers, whose comments and suggestions have notably improved the manuscript. This work was funded by CNR-Istituto di Geoscienze e Georisorse-sezione di Firenze, by MIUR, PRIN 2005, project "Complexity in minerals: modulation, modularity, structural

disorder'' and by University of Bari (Fondi Ateneo ex 60%, 202160133).

Appendix A. Supplementary Materials

Supplementary data associated with this article can be found in the online version at doi:10.1016/j.jssc.2007.11.032.

References

[1] M. Zelenski, T. Balić-Žunić, L. Bindi, A. Garavelli, E. Makovicky, D. Pinto, F. Vurro, Am. Mineral. 91 (2006) 21–28.
[2] Y. Moëlo, E. Makovicky, N.N. Mozgova, J.L. Jambor, N. Cook, A. Pring, W. Paar, E.H. Nickel, S. Graeser, S. Karup-Møller, T. Balić-Žunić, W.G. Mumme, F. Vurro, D. Topa, L. Bindi, K. Bente, M. Shimizu, Eur. J. Mineral. 20 (2008), in press.
[3] H. Strunz, E.H. Nickel, Strunz Mineralogical Tables. Chemical-Structural Mineral Classification System, ninth ed, Schweizerbart, Stuttgart, Germany, 2001, p. 870.
[4] W.G. Mumme, E.H. Nickel, Am. Mineral. 72 (1987) 1257–1262.
[5] B. Mason, W.G. Mumme, H. Sarp, Am. Mineral. 77 (1992) 197–200.
[6] Oxford Diffraction, CrysAlis CCD and RED, Version 1.70, Oxford Diffraction Ltd., Oxford, UK, 2002.
[7] R.H. Blessing, Acta Crystallogr. A 51 (1995) 33–38.
[8] G.M. Sheldrick, SHELXS-97, A Program for Crystal Structure Refinement, University of Göttingen, Germany, 1997.
[9] G.M. Sheldrick, SHELXS-97, A Program for Automatic Solution of Crystal Structures, University of Göttingen, Germany, 1997.
[10] C.K. Johnson, H.A. Levy, in: J.A. Ibers, W.C. Hamilton (Eds.), International Tables for X-ray Crystallography, vol. IV, Kynoch Press, Birmingham, 1974, pp. 311–336.
[11] Ju.Z. Nozik, L.E. Fykin, L.A. Muradjan, Kristallografiya 21 (1976) 76–79.
[12] R.W.G. Wyckoff, Crystal Structures, second ed., Interscience Publishers, New York, NY, 1963, pp. 239–444.
[13] R.W.G. Wyckoff, Crystal Structures, second ed., Interscience Publishers, New York, NY, 1963, pp. 298–306.
[14] L.-Q. Fan, Y.-Z. HuanG, L.-M. Wu, L. Chen, J.-Q. Li, J. Ma En, Solid State Chem. 179 (2006) 2361–2366.
[15] N.V. Pervukhina, V.I. Vasil'ev, D.YU. Naumov, S.V. Borisov, S.A. Magarill, Can. Mineral. 42 (2004) 87–94.
[16] N.V. Pervukhina, V.I. Vasil'ev, S.V. Borisov, S.A. Magarill, D.YU. Naumov, Can. Mineral. 41 (2003) 1445–1453.
[17] T. Balić-Žunić, E. Makovicky, Acta Crystallogr. B 52 (1996) 78–81.
[18] E. Makovicky, T. Balić-Žunić, Acta Crystallogr. B 54 (1998) 766–773.
[19] T. Balić-Žunić, I. Vicković, J. Appl. Crystallogr. 29 (1996) 305–306.
[20] N.E. Brese, M. O'Keeffe, Acta Crystallogr. B 47 (1991) 192–197.